JTTEE5 11:359-364

High Temperature Damping Behavior of Plasma Sprayed NiCoCrAlY Coatings

K.A. Khor, C.T. Chia, Y.W. Gu, and F.Y.C. Boey

(Submitted 9 November 2001; in revised form 20 February 2001)

There is a trend to design the turbine coating and the substrate as in integral, layered, engineering assembly. Under the harsh environment of the turbine engine, a failure in one component can quickly lead to failure in other components. Materials that are used in structural applications are prone to mechanical vibration, which, when not attenuated, will lead to fatigue of components and shortening of life cycle. Therefore, it is necessary to examine the thermal stability and dynamic mechanical properties of coatings under dynamic conditions. In addition to these noise reduction and vibration amplitude control motivated objectives, however, mechanical energy dissipation processes also find intrinsic applications in cases for which a thorough understanding of the mechanisms responsible for the damping response of the material is required. This article describes the damping behavior and mechanisms that exist in plasma sprayed NiCoCrAlY coatings.

Keywords creep, damping behavior, dislocations, NiCoCrAlY, plasma spray, thermal barrier coatings

1. Introduction

High damping structural materials have the potential to greatly reduce vibration and noise in many types of mechanical systems. The deposition of thermal barrier coatings may provide some form of passive damping to the structural materials. This is important because additional machinery or attachments to provide damping to the structural material will definitely increase the material's load, which is critical in anaero-propulsion system.[1,2]

However, a basic understanding about the origins of the damping mechanisms is also important for optimization and control purposes. In the worst case, measurements made over a range of frequencies or temperatures may represent the overlapping contributions of a number of unknown damping mechanisms, and thus measurements may be impossible to interpret in any meaningful manner. At the other extreme, a material may exhibit one or more well-resolved internal friction peaks, each of which originates from a specific damping mechanism.

This article describes the measurement of the dynamic mechanical properties of NiCoCrAlY bond coat using a dynamic mechanical analyzer (DMA). To further understand what mechanisms are responsible for the increasing high temperature background, microstructure characterization by scanning electron microscopy (SEM), x-ray diffraction (XRD), and mercury-intrusion porosimetry were used to quantify the influence of microstructure on the dynamic mechanical properties. The probable high temperature damping mechanisms are discussed in light of the experimental results.

K.A. Khor, C.T. Chia, Y.W. Gu, School of Mechanical Production Engineering, Nanyang Technological University, Nanyang Avenue, Singapore 639798; and **F.Y.C. Boey,** School of Materials Engineering, Nanyang Technological University, Nanyang Avenue, Singapore 639798. Contact e-mail: mkakhor@ntu.edu.sg.

Table 1 Plasma Spraying Parameters

Plasma Gun	SG-100 (Miller Therm, Inc., Indianapolis, IN)
Net energy, kW	17.7
Argon gas, m^3/h	2.32
Helium gas, m^3/h	1.13
Carrier gas, m^3/h	0.34
Feed rate, g/min	35

2. Experimental Procedure

2.1 Plasma Spraying and Sample Preparation

The NiCoCrAlY powders were directly used as feedstock for plasma spraying (Table 1) onto an aluminum substrate. The coating was deposited to a thickness of about 600 μm. The as-sprayed coatings were then cut from the substrate with a diamond cutter to create freestanding coatings. The coatings were then annealed in air at 900 °C for 4 h, to relieve stress and aid in homogenization. The coatings were then finished to the size of 8 × 4.5 × 0.25 mm using fine grade SiC paper. All specimens were flat and opposite surfaces across the length, thickness, and width were parallel to within 0.1%, in accordance with ASTM standard E1875-97.[3]

2.2 Microstructural Characterization

An optical microscope and JSM-5600LV scanning electron microscope (JEOL, Tokyo, Japan) attached with an energy dispersive x-ray spectrometer (EDS) were used to study the microstructure of the coatings, and chemical composition of coatings and oxide stringers. XRD analysis was carried out to determine the phases present prior to the dynamic mechanical analysis. The AutoPore III mercury porosimeter (Micromeritics, Norcross,

GA) was used to determine the pore size distribution and total pore volume. The porosimeter is capable of measuring pore diameters in the range of 0.003-360 μm. The grain size of the γ phase was measured by the Pro-image software (Leica, Cambridge, UK).

2.3 DMA

2.3.1 Temperature Scan Mode. The tests were carried out in the temperature scan mode with a three-point bending measuring system. The temperature range was set from 30-950 °C at a heating rate of 10 °C·min^{-1} and was checked through a thermocouple wire placed adjacent to the test specimen. The oscillation frequencies were set at 0.1, 1, and 5 Hz. The sample was subjected to a static force of 1000 mN and a dynamic force of 666.7 mN. This load was well within the elastic limit of the coatings so that the effects of nonlinear stress distribution within the coatings could be minimized. The accuracy of the DMA measurement was calibrated following manufacturer's instructions.

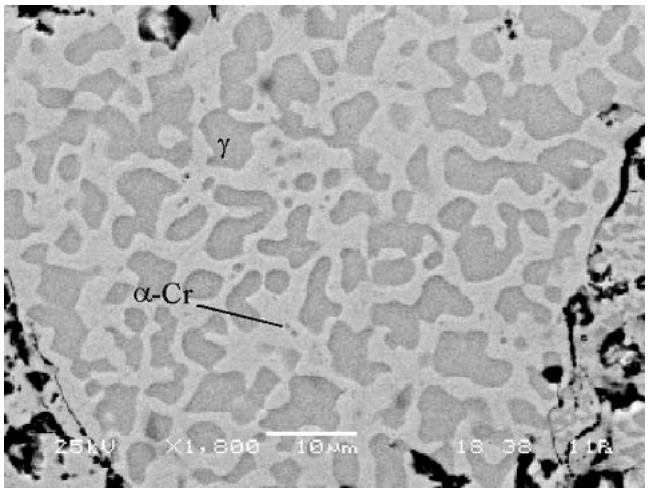

Fig. 1 SEM image of etched NiCoCrAlY coating

2.3.2 Quasi-Static Creep Test. The creep test was performed to further elucidate whether the anelastic or viscoelastic effect governed the creep process above 700 °C. The test was performed at 750, 800, and 850 °C. Each specimen was subjected to four to six separate creep-relaxation tests, with each successive loading at a stress level twice that of the previous one. The specimens were loaded at different stress level of 1.5, 15, 30, 60, and 120 MPa. The strain versus time plot was recorded.

3. Results

3.1 Microstructural Characterization

Figure 1 shows the microstructure of an etched NiCoCrAlY bond coating. There are open porosity, oxide stringers (Al_2O_3), and interlamellar flake-like pores. The structure of the bond coat layer itself consists of two phases: γ-face-centered cubic (fcc) (Ni-Cr-Co-Al rich solid solution, gray area) and α-Cr body-centered cubic (bcc) (Cr-Co-Al rich solid solution, white area). The γ-phase appears as an isolated phase separated by the continuous α-Cr phase. The x-ray diffraction diagram is shown in Fig. 2.

The mercury-intrusion porosimeter (MIP) was used to characterize the pore size and pore distribution. Figure 3 shows the results of the MIP test for annealed NiCoCrAlY coating. The result shows that there are two characteristic and narrow zones of pore sizes contributing mostly to the open porosity of plasma sprayed material. The two types of pores are mesopores and micropores.[4] Mesopores in coatings are capable of attaining a size range of 30-100 μm, and the micropores with dimension of 0.1-1 μm can be observed in the annealed NiCoCrAlY case.

To further quantify the grain size of the γ-phase in the NiCoCrAlY layers, SEM images of the etched samples were analyzed using Pro-image software. The results are shown in Table 2.

3.2 The Dynamic Mechanical Properties of Annealed NiCoCrAlY Coating

The dynamic mechanical properties of annealed NiCoCrAlY are shown in Fig. 4. The continuous increase of internal friction

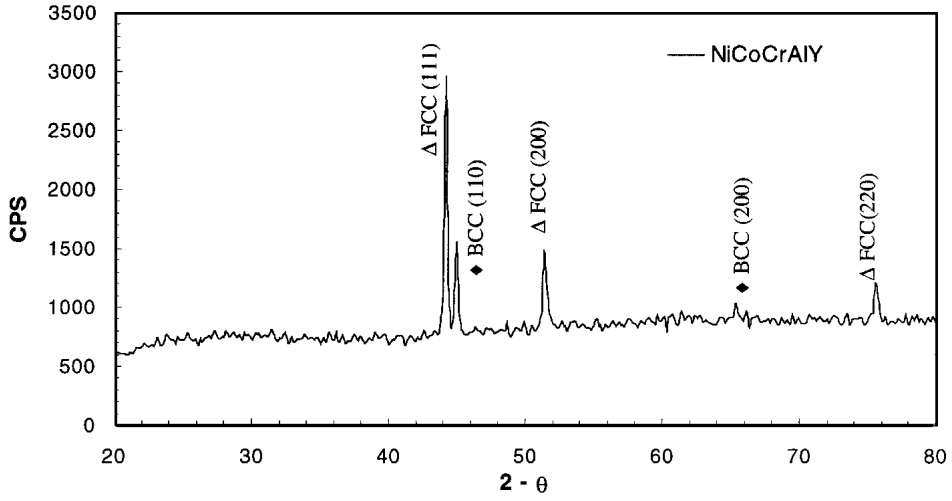

Fig. 2 XRD patterns of annealed NiCoCrAlY coating: △, γ; ◆, α-Cr

(damping factor) with increasing temperature has been known as high-temperature background. The magnitude of this high-temperature background is also known as highly structure sensitive.[5]

However, a lack of a detectable relaxation peak leaves unanswered the question of whether anelasticity or linear viscoelasticity is involved. To account for the form of the high-temperature background in the purely anelastic nature would require a broad spectrum of relaxation times that increases monotonically and without a detectable limit with increasing values of relaxation time τ that is expressible by an Arrhenius equation

$$\tau = \tau_0 \exp\left(\frac{Q}{kT}\right) \quad \text{(Eq 1)}$$

where T is the absolute temperature, τ_0 is a time factor, Q is the activation energy, and k is the gas constant. Fortunately, the speculation about the anelastic or viscoelastic nature of the mechanisms producing the high-temperature background is answerable experimentally through the use of quasi-static experiments.

Table 2 Grain Size Characterization of γ Phase

Phase	Area Ratio = $Area_{phase}/Area_{total}$	Size Distribution
γ	45.24 ± 5.25%	4.86 ± 3.19 μm

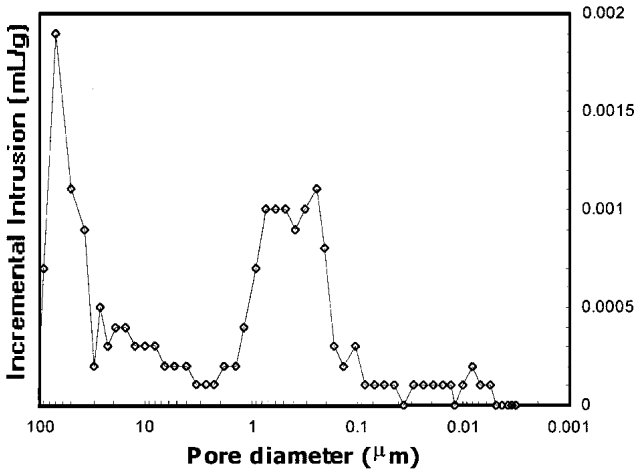

Fig. 3 Pore size distribution of annealed NiCoCrAlY coating by mercury-intrusion porosimetry

3.3 Quasi-Static Test (Creep Test) of Annealed NiCoCrAlY Coating

Figure 5(a-c), shows the creep test for annealed NiCoCrAlY coating for four different stress levels (1.5, 15, 30, 60, and 120 MPa) at temperatures of 750, 800, and 850 °C. The strain versus time curves illustrate that during the initial creep test, the sample's strain increased almost instantly and was followed by a constant strain rate region with no indication of reaching a limit. After the load was removed, the sample responded instantaneously with a very sharp drop in strain value. A decreasing trend in the strain value again follows this change. However, the strain does not reach the original zero deflection position even after 60 min. This is strong evidence that a diffusion mechanism is not fully responsible for the increasing high temperature background. Instead, a viscoelastic behavior is observed for the annealed NiCoCrAlY coating.

4. Discussion

A review of the literature shows that there are a couple of mechanisms that can possibly be influencing the damping be-

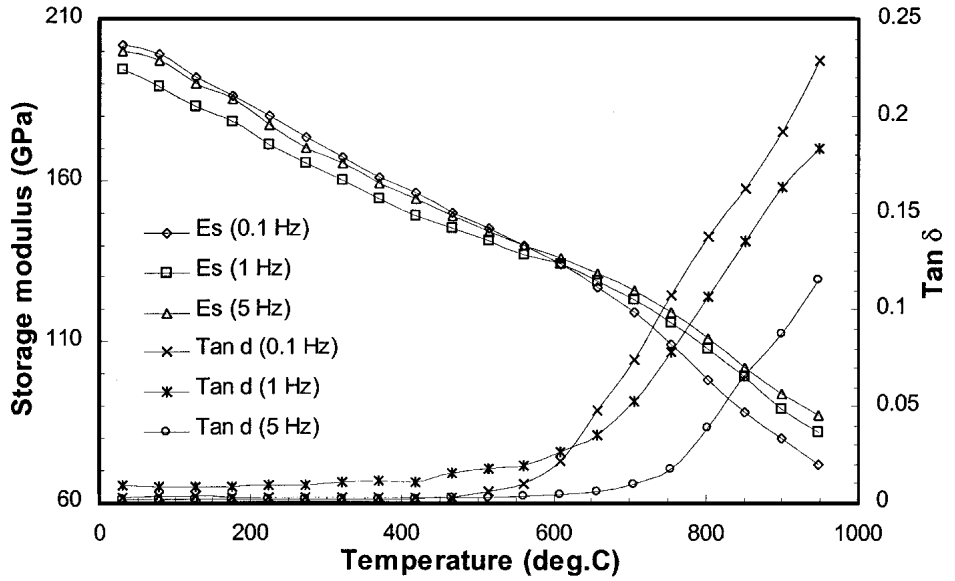

Fig. 4 The dynamic mechanical properties of an annealed NiCoCrAlY coating. The dynamic storage modulus is a measure of the material's ability to store energy and is commonly used for an indication of interatomic potential. Damping is one of the most sensitive measures of atomic motion, and is particularly suitable for the evaluation of structural relaxation activated by the thermal process. Tan δ is the damping factor.

havior of the NiCoCrAlY coating. The crystallographic defects that influence damping mechanisms and are important in metals and alloys include point defects (vacancies and interstitial), line defects (dislocations), surface defects (grain boundaries and interfaces) and bulk defects (micropores and microcracks). In plasma sprayed coatings, point defect damping is essentially small relative to other sources of damping, and therefore is excluded.[5,6] The following discussion will address the experimental results and its relation to the damping mechanisms operative in the NiCoCrAlY bond coatings.

4.1 Dislocation Damping Mechanism

In typical plasma sprayed NiCoCrAlY coatings, there are many small regions of oxide stringers being formed during the plasma spraying process. The thermal coefficients of expansion (CTE) of these flake-like oxide stringers are different from the NiCoCrAlY matrix. The difference between the CTE values is likely to result in increased dislocation density at the interfaces during cooling and solidification of plasma spray coatings.

Material damping is related to dislocations by the following equation:

$$Q^{-1} = \frac{C_1}{\varepsilon_0} \exp\left(-\frac{C_2}{\varepsilon_0}\right) \qquad \text{(Eq 2)}$$

where Q^{-1} is the dislocation damping and C_1 and C_2 are material constants; C_1 is proportional to dislocation density in the matrix.[7-10] Figure 6(a-d) show the plots of log $(Q^{-1}\varepsilon_0)$ versus $1/\varepsilon_0$ for the four temperatures ranging from 400-700 °C. It is observed that at in the $1/\varepsilon_0$ range of 3700-4500, the plot is a straight line. This lends support to the presence of a damping mechanism by dislocation. There is, however, deviation in this relationship at low $1/\varepsilon_0$ values, indicating that other mechanisms are counteracting this relationship.

4.2 Grain Boundary Damping Mechanism

Damping mechanism by grain boundary relaxation, anelasticity, or viscoelasticity in polycrystalline metals or alloys has been studied extensively by Ke[11] and Zener.[12] In polycrystalline alloys, the viscous sliding could occur between two adjacent crystals. According to Zener's prediction, the shear stress that initially acts across a boundary is gradually reduced through viscous slip while the grains corners sustain more and more of the total shearing force. The energy absorbed at grain boundaries is dependent on the magnitude of the shear stress and the grain boundary area per unit volume, i.e., grain size. To evaluate the effect of grain size on the level of damping, the damping factor of as-spray and annealed coatings was plotted against temperature (Fig. 7). The as-sprayed coating consists of partial amorphous and nanocrystalline grain in direct contrast to the annealed NiCoCrAlY sample (having a grain size ≈ 4.86 ± 3.19 μm). The reason for the selection of these two samples for comparison is obvious when one remembers the increase in grain boundary area with a decrease of grain size. Therefore, one would expect the total grain boundary surface area of as-sprayed coatings to be larger than that of large grain size annealed coatings.

From Fig. 7, it can be observed that the damping factor of the as-sprayed NiCoCrAlY coating is higher than that of the annealed coating. This is strong evidence for the increase of damping factor with decreasing grain size or increasing grain boundary area. The grain boundary damping mechanism was prevalent until about 750 °C, when the two damping curves merged. This demonstrated that another mechanism is dominating the process.

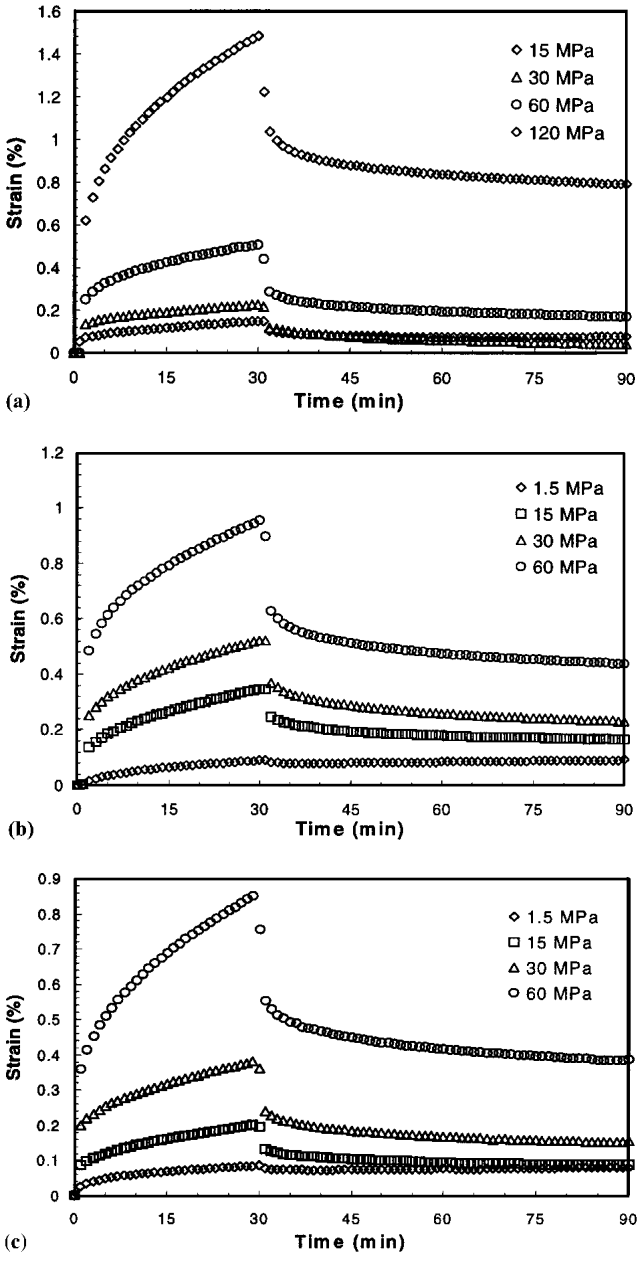

Fig. 5 **(a)** Creep test results at 750 °C. **(b)** Creep test results at 800 °C. **(c)** Creep test results at 850 °C

4.3 Interface Damping Mechanism

The plasma sprayed NiCoCrAlY bond coat contains a weakly bonded interface between oxide stringer and NiCoCrAlY matrix layers.[13] The weakly bonded interface may be inferred not only from the SEM image as shown in Fig. 3, but

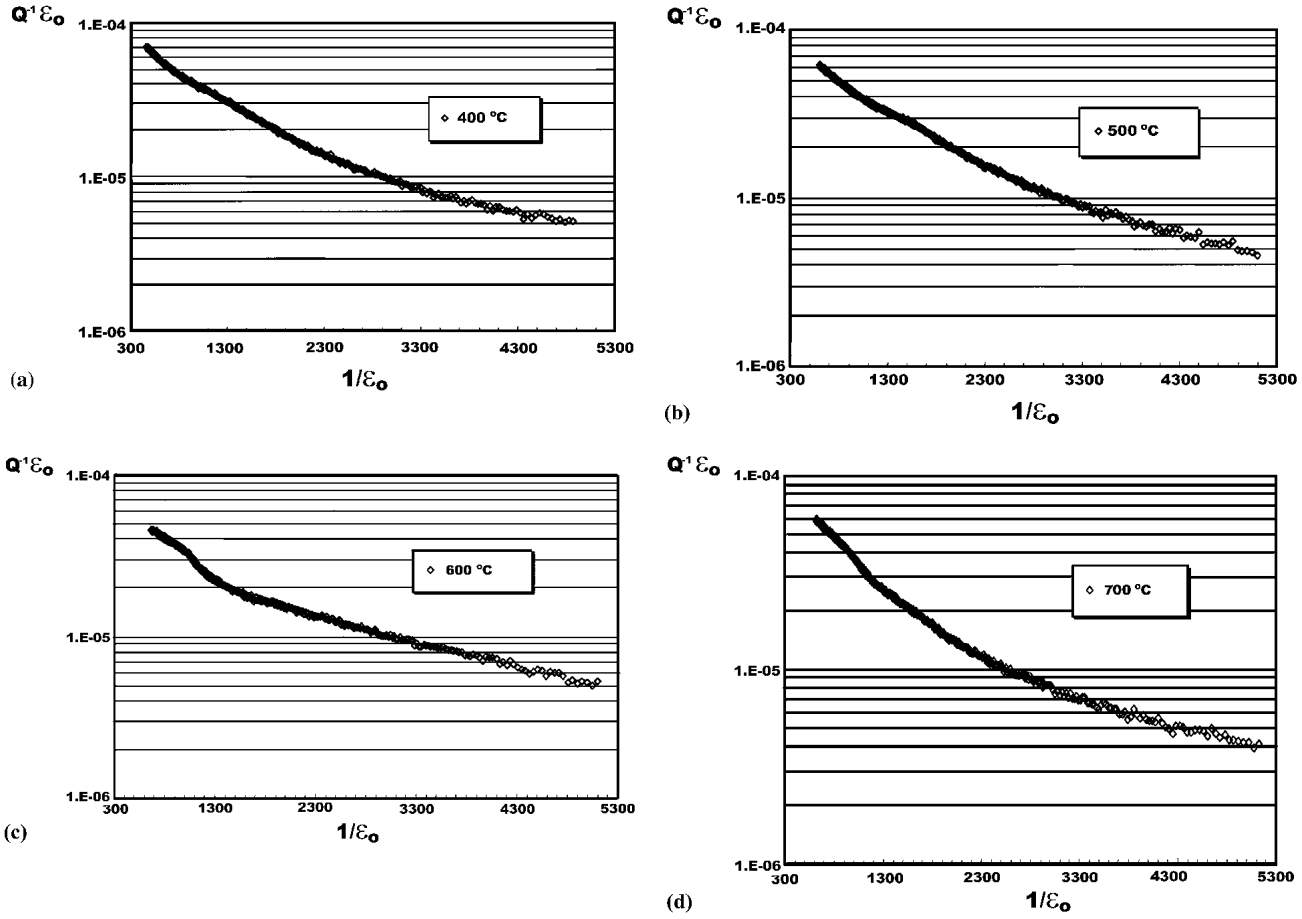

Fig. 6 **(a)** Plot of log ($Q^{-1}\varepsilon_0$) versus $1/\varepsilon_0$ at 400 °C. **(b)** Plot of log ($Q^{-1}\varepsilon_0$) versus $1/\varepsilon_0$ at 500 °C. **(c)** Plot of log ($Q^{-1}\varepsilon_0$) versus $1/\varepsilon_0$ at 600 °C. **(d)** Plot of log ($Q^{-1}\varepsilon_0$) versus $1/\varepsilon_0$ at 700 °C

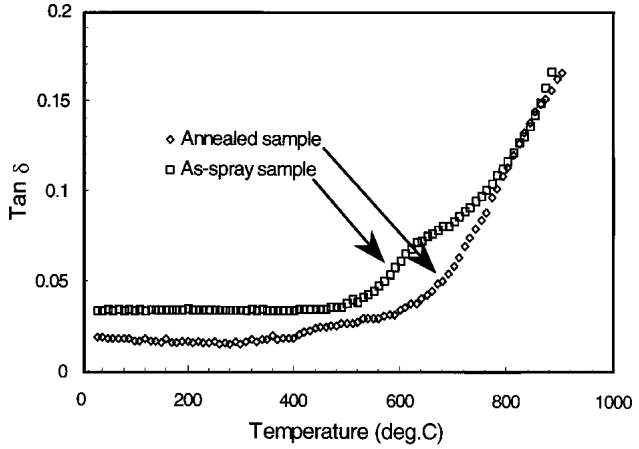

Fig. 7 Comparison of the damping factor of as-spray and annealed NiCoCrAlY coatings

also from the mercury intrusion porosimeter measurement (Fig. 5) showing micropores at the interface between lamellae. Even in regions of the oxide stringer/NiCoCrAlY matrix interface where there is no porosity present, interfacial bonding is likely to be weak because of the layered surface structure that is present in the flake oxide stringers. This is in agreement with other reported observations on lamella interfaces.[14-16] As the temperature increases, the interface effect becomes significant because the NiCoCrAlY matrix softens relative to the Al_2O_3 oxide stringers and a reversible movement at the interfaces is likely to occur. On the basis of these considerations, interfacial slip is likely to occur at the interfaces when the samples are in the nonuniform stress state under bending mode.

4.4 Summation of Damping Mechanisms

In consideration of the different damping mechanisms discussed thus far, it is appropriate to sum all of the damping sources of plasma sprayed coating as

$$\text{Tan } \delta_{\text{Total}} = \tan \delta_{\text{diffusion}} + \tan \delta_{\text{dislocation}} + \tan \delta_{\text{grain boundary}} + \tan \delta_{\text{interfacial}} \quad \text{(Eq 3)}$$

5. Conclusions

The damping capacity of plasma sprayed NiCoCrAlY bond coat for substrate coating has been shown to exhibit significant damping gains both at ambient and high temperatures. It is observed that the thermal barrier coating itself can provide a chan-

nel for the attenuation of vibration and noise, which is prevalent in the turbulent environment of a turbine engine.

The damping mechanisms associated with plasma sprayed coatings can be expressed as a summation of the aforementioned damping mechanisms. For the temperature range 30-700 °C, the possible dominant damping mechanisms are diffusion, dislocation damping, and oxide stringer/matrix interface damping. On the other hand, above 700 °C, grain boundary sliding, interface sliding friction, and debonding are likely to be responsible for a large portion of the observed damping.

Acknowledgment

The authors would like to thank the support of the School of Mechanical and Production Engineering, Nanyang Technological University, Singapore, in the form of research grants RP 56/92 and RG 25/96.

References

1. A.D. Nashif: "Application of Damping for Noise Control in Diesel Engine Components" in *Damping Applications for Vibration Control*, P.J. Torvik, ed., The Winter Annual Meeting of the American Society of Mechanical Engineers, ASME, Chicago, IL, 1980, pp. 133-44.
2. J.P. Henderson: "Damping Applications in Aero-Propulsion Systems" in *Damping Applications for Vibration Control*, P.J. Torvik, ed., The Winter Annual Meeting of the American Society of Mechanical Engineers, ASME, Chicago, IL, 1980, pp. 145-58.
3. ASTM E1875-97, *Dynamic Young's Modulus, Shear Modulus, and Poisson's Ratio by Sonic Resonance*, American Society for Testing and Materials, Philadelphia, PA, 1997.
4. L. Pawlowski: The *Science and Engineering of Thermal Spray Coatings*, John Wiley & Sons, New York, 1995.
5. A.S. Nowick and B.S. Berry: *Anelastic Relaxation in Crystalline Solids*, Academic Press, New York, 1972, pp. 147-61.
6. R. De Batist: *Internal Friction of Structural Defects in Crystalline Solids*, North-Holland Publishing, Amsterdam, 1972, pp. 36-445.
7. A. Granato and K. Lucke: "Theory of Mechanical Damping Due to Dislocations," *J. Appl. Phys.*, 1956, *27*(6), pp. 583-93.
8. M. Vogelsang, R.J. Arsenault, and R.M. Fisher: "An In Situ HVEM Study of Dislocation Generation at Al/SiC Interfaces in Metal Matrix Composites," *Metall. Trans. A*, 1986, *17A*, pp. 379-89.
9. D. Dunand and A. Mortensen: "Thermal Mismatch Dislocations Produced by Large Particles in a Strain-Hardening Matrix," *Mater. Sci. Eng. A*, 1991, *135*, pp. 179-84.
10. J. Zhang, R.J. Perez, and E.J. Lavernia: "Dislocation-Induced Damping in Metal Matrix Composites," *J. Mater. Sci.*, 1993, *28*, pp. 835-46.
11. T.S. Ke: "Stress Relaxation Across Grain Boundaries in Metals," *Phys. Rev.*, 1947, *72*, pp. 41-46.
12. C. Zener: *Elasticity and Anelasticity of Metals*, The University of Chicago Press, Chicago, 1948, pp. 147-59.
13. R. McPherson: "A Review of Microstructure and Properties of Plasma Sprayed Ceramic Coatings," *Surf. Coat. Technol.*, 1989, *39/40*, pp. 173-81.
14. C.J. Li, A. Ohmori, and R. McPherson: "The Relationship Between Microstructure and Young's Modulus of Thermally Sprayed Ceramic Coatings," *J. Mater. Sci.*, 1997, *32*, pp. 1004-11.
15. A. Ohmori and C.J. Li: "Quantitative Characterization of the Structure of Plasma-Sprayed Al_2O_3 Coating by Using Copper Electroplating," *Thin Solid Films*, 1991, *201*, pp. 241-52.
16. R. McPherson and P. Cheang: "Elastic Anisotropy of APS Alumina Coatings and Its Relationship to Microstructure" in *High Performance Ceramic Film and Coatings*, P. Vincenzini, ed., Elsevier Science, Amsterdam, 1990, pp. 277-90.